



Article

Assessing the Water Budget Closure Accuracy of Satellite/Reanalysis-Based Hydrological Data Products over Mainland China

Zengliang Luo^{1,2,3}, Han Yu^{2,3}, Huan Liu^{4,*} and Jie Chen¹

¹ State Key Laboratory of Water Resources Engineering and Management, Wuhan University, Wuhan 430072, China; luozengliang@cug.edu.cn (Z.L.); jiechen@whu.edu.cn (J.C.)

² Key Laboratory of Regional Ecology and Environmental Change, School of Geography and Information Engineering, China University of Geosciences, Wuhan 430074, China; chopin@cug.edu.cn

³ State Key Laboratory of Biogeology and Environmental Geology, China University of Geosciences, Wuhan 430074, China

⁴ China Institute of Water Resources and Hydropower Research (IWHR), Beijing 100038, China

* Correspondence: liuhuan@iwhr.com

Abstract: A good water budget involving four variables, including precipitation (P), evapotranspiration (ET), streamflow (R), and terrestrial water storage change ($TWSC$), is reflected in two aspects: a high accuracy against observations for each budget component and the low water budget closure residual error (ΔRes). Due to the lack of consideration of observations of budget components in existing water budget closure assessment methods ($BCMs$), when the ΔRes of budget components is low, their error against respective observations may still be high. In this study, we assess the water budget closure accuracy of satellite/reanalysis-based hydrological data products over mainland China based on six popular P products and multiple datasets of additional budget components (ET , R , and $TWSC$). The results indicated that the ΔRes changes between ± 15 mm over mainland China. Satellite P products such as $GPM\ IMERG$ showed better performance by comparing them with rain gauge-based observations. However, reanalysis P products such as $GLDAS$ and $FLDAS$ showed a better water budget closure since the selected datasets of additional budget components (ET and R) are also derived from reanalysis datasets. This indicates that these same data sources for budget components make it easier to close the water budget. The further development of satellite P products should consider the closure of the water budget with other water cycle variables.

Keywords: precipitation products; water budget closure; hydrological cycle; mainland China



Citation: Luo, Z.; Yu, H.; Liu, H.; Chen, J. Assessing the Water Budget Closure Accuracy of Satellite/Reanalysis-Based Hydrological Data Products over Mainland China. *Remote Sens.* **2023**, *15*, 5230. <https://doi.org/10.3390/rs15215230>

Academic Editor: Luca Brocca

Received: 6 October 2023

Revised: 31 October 2023

Accepted: 1 November 2023

Published: 3 November 2023



Copyright: © 2023 by the authors. Licensee MDPI, Basel, Switzerland. This article is an open access article distributed under the terms and conditions of the Creative Commons Attribution (CC BY) license (<https://creativecommons.org/licenses/by/4.0/>).

1. Introduction

Precipitation (P) is the main driver of the terrestrial hydrological cycle [1–3]. A great number of satellite and reanalysis precipitation (SRP) products, characterized by global coverage and high temporal and spatial resolution, have been produced and widely applied in large-scale meteorological and hydrological analyses [4–7]. This is because, despite the high accuracy of in situ rainfall observations, they are sparse, and the record length in many basins around the world is insufficient, limiting the accuracy of hydrological research in these basins greatly [8]. Despite the advantages of SRP products over rain gauge-based observations in terms of spatial coverage and resolution, they have large uncertainties and errors arising from sensor deficiencies, retrieval algorithms, and discordant data resolution [9–11]. More importantly, the water budget closure accuracy of SRP products with respect to products of additional budget components (ET , R , and $TWSC$), which is critical for accurate hydrological research, may be low. Therefore, when studying hydrological changes in regional and global basins, the products of hydrological variables should meet high accuracy targets in two aspects, i.e., the high accuracy against observations for each budget component and the low water budget closure residual error.

In the literature, the assessment of water budget closures has become a basic condition for verifying the reliability of hydrological products [12–15]. Water budget closure-based assessment methods (*BCMs*) help users understand the error sources and uncertainties of budget component datasets by quantifying water budget imbalances [16,17]. The residual error in water budget closure $\Delta Res = P - ET - R - TWSC$ has been commonly used to assess the water budget imbalance caused by errors in budget component datasets [13,18,19]. Based on ΔRes , a series of derived methods (*BCMs*) have been developed; they include the proportion of ΔRes to mean precipitation and the method for closing water and energy budgets, simultaneously developed by Hobeichi et al. [20]. Sheffield et al. [9] assess the ability of remote sensing products of P , ET , and $TWSC$ to close water budget by comparing their residual error represented by the estimated R ($R = P - ET - TWSC$) with streamflow observations; Lehmann et al. [21] assess water budget closure of budget component datasets by using the estimated $TWSC$ as the residual error, and then the estimated $TWSC$ was compared with the measured $TWSC$ using the Gravity Recovery And Climate Experiment (*GRACE*) satellite mission. However, these *BCMs* lack consideration of observations of budget components when assessing the water budget accuracy of budget component products and are subject to mutual cancellation of errors in budget component products from different sources, which was defined as the high accuracy of water budget closure but the low accuracy of individual budget components in this study. As a result, the accuracy of the selected budget component products (against observations) based on *BCMs* may be low, although the ΔRes of these selected datasets is small. The combination of existing *BCMs* and observations of budget components provides an opportunity to solve this problem.

Many studies have been conducted to assess how existing hydrological products can close water budgets in different global basins since different products of budget components show various accuracies in different regions [22,23]. Abolafia-Rosenzweig et al. [24] evaluated three techniques: proportional redistribution, constrained Kalman filter, and multiple collocations for enforcing water budget closure in 24 global basins. Luo et al. [12] proposed a novel error-based method for assessing the water budget closure of satellite-based hydrological products in the Tarim River Basin, and Soltani et al. [18] proposed a probabilistic framework for estimating water budgets in low runoff regions of the central Basin of Iran. Sahoo et al. [25] use the $\Delta Res/P$ to assess the water budget closure accuracy of satellite remote sensing data of budget components in ten global basins and found that the $\Delta Res/P$ is changed between 5 and 25% in most basins. Different studies in different basins showed various water budget closure accuracies due to the diverse inversion accuracy of hydrological products in these basins. There is currently no relevant report on the question of how satellite/reanalysis-based hydrological products can close the terrestrial water budget over mainland China.

Based on the above analysis, *BCMs* have the advantage of quantifying the water budget closure of *SRP* products with respect to datasets of additional budget components but are subject to the mutual cancellation of errors in budget components. Maintaining a high precision in budget component datasets in both aspects of against observations and water budget closure is critical for accurate hydrological research. Statistical metrics, such as root mean square error, correlation coefficient, and false alarm ratio, were commonly used to assess *SRP* products by comparing them with rain gauge-based observations [26]. If high-precision datasets can be pre-selected using statistical metrics and then the selected datasets are applied to *BCMs*, it is possible that *SRP* products based on existing *BCMs* have high accuracy in the two aspects mentioned above. Therefore, this study focuses on assessing and intercomparing the water budget closure accuracy of six popular *SRP* products relative to datasets of additional budget components in mainland China by combining statistical methods and existing *BCMs*. The assessment helps understand the water budget closure state of existing hydrological products in mainland China. In detail, the statistical methods were first used to quantify the accuracy of *SRP* products by comparing them with rain gauge-based observations to ensure that the accuracy of *SRP* products applied to water

budget closure assessment is high. The existing *BCMs* were then used to quantify the ΔRes of the selected *SRP* products with respect to datasets of additional budget components.

The specific objectives of this study were: (1) to assess the water budget closure accuracy of six popular *SRP* products relative to the selected datasets of additional budget components in mainland China. The difference in closing water budget between satellite and reanalysis *P* products is further investigated due to their different inversion methods; (2) to compare the difference in *SRP* assessment between statistical methods and *BCMs* with mainland China as a case study; and (3) to investigate the uncertainties that affect *SRP* assessment.

This study was organized as follows. Study area and data are described in Section 2.1 and Section 2.2; Methods used in this study are represented in Section 2.3; Results for assessing *SRP* products and intercomparing their accuracies for closing water budget are presented in Section 3; The main results and uncertainties affecting water budget closure assessment are discussed in Section 4; Finally, the conclusions are summarized in Section 5.

2. Study Area, Datasets, and Methodology

2.1. Study Area

Figure 1a, b shows the study area of mainland China, with an area of approximately 9.6 million km². It covers diverse topography and climatic regions, indicating that the performance of *SRP* products in different topographies and climatic conditions can be well investigated with mainland China as a case study. The mean annual *P* across mainland China ranges from 7 to 2754 mm [27]. It decreases significantly from the southeast to northwest of mainland China and is affected by the prevailing monsoon climate from the Indian and Pacific Oceans [28]. As shown in Figure 1a, rain gauge stations within mainland China are mainly distributed in eastern China and less distributed in western China, covered mainly by desert and alpine landscapes.

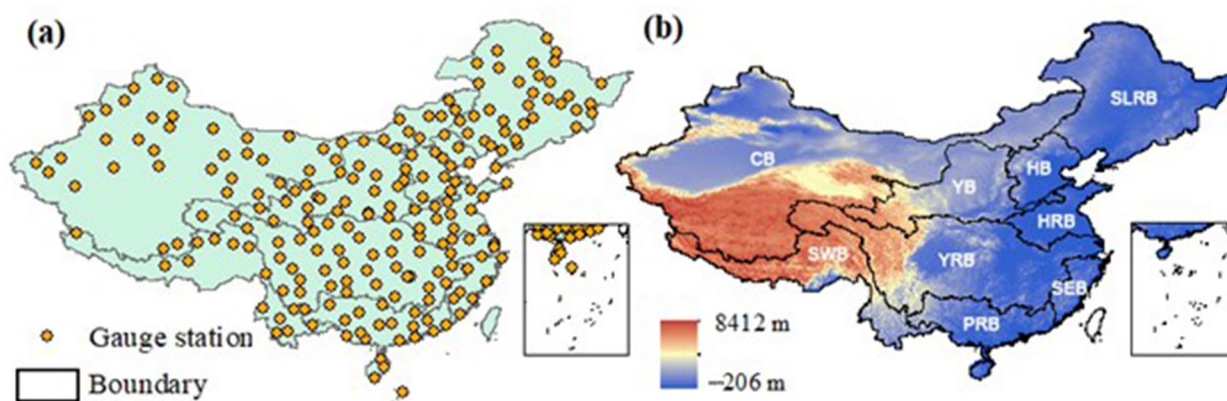


Figure 1. Study area of mainland China. (a) Rain gauge stations that were used in this study; (b) DEM and nine major basins in mainland China, including the Songhua and Liaohe River Basin (SLRB), Haihe River Basin (HB), Huaihe River Basin (HRB), Yellow River Basin (YB), Yangtze River Basin (YRB), Pearl River Basin (PRB), Southeast Basin (SEB), Southwest Basin (SWB), and Continental Basin (CB).

2.2. Datasets

2.2.1. Rain Gauge Observations

A monthly ground-station dataset of precipitation derived from the China Meteorological Data Service Center (<http://data.cma.cn/en> (accessed on 31 October 2023)) was used as the reference for assessing the accuracy of *SRP* products. Locations of rain gauge stations used in this study are shown in Figure 1a. These data were collected from 2000 to 2020. In order to ensure the quality of data, many rain gauge stations with a large number of missing values were removed. In detail, we use 5% as a threshold to filter rain gauge stations. That is, rain gauge stations with the amount of missing data accounting for less

than 5% of these total data, which means that the overall evaluation performance will not be affected by missing data, were selected; for the selected rain gauge stations, months with no data during the study period were interpolated using a sample linear interpolation method.

2.2.2. SRP Products

Table 1 shows the SRP products used in this study: *GPM IMERG*, *TRMM 3B43*, *PERSIANN-CDR*, *ERA5*, *GLDAS*, and *FLDAS*. They include different data sources and inversion algorithms and have been widely used for hydrological analysis in previous studies [29,30]. Figure 2 shows the spatial distribution of these six SRP products.

Table 1. Features of the selected six popular precipitation products.

Precipitation Product	Resolution	Period	Provider	Reference
Monthly Global Precipitation Measurement (GPM) v6 (GPM IMERG)	0.1 degree 3 h	2000–present	NASA GES DISC at NASA Goddard Space Flight Center, Maryland, United States	Huffman et al. 2019 [31]
TRMM (TMPA/3B43) Rainfall Estimate L3 (TRMM 3B43)	0.25 degree 1 month	1998–2019	NASA GES DISC at NASA Goddard Space Flight Center, Maryland, United States	Huffman et al 2010 [32]
NOAA Climate Data Record (CDR) of Precipitation Estimation from Remotely Sensed Information using Artificial Neural Networks (PERSIANN-CDR), Version 1 Revision 1 (PERSIANN-CDR)	0.25 degree 1 day	1983–present	NOAA NCDC, North Carolina, United States	Sorooshian et al. 2014 [33]
The fifth generation ECMWF atmospheric reanalysis of the global climate (ERA5)	0.25 degree 1 month	1979–present	ECMWF/Copernicus Climate Change Service, Reading, United Kingdom	Copernicus Climate Change Service, 2017 [34]
GLDAS Noah Land Surface Model L4 (GLDAS)	0.25 degree 3 h	2000–present	NASA GES DISC at NASA Goddard Space Flight Center, Maryland, United States	Rodell et al. 2004 [35]
FLDAS Noah Land Surface Model L4 (FLDAS)	0.10 degree 1 month	1982–present	NASA GES DISC at NASA Goddard Space Flight Center, Maryland, United States	McNally et al. 2017 [36]

The *GPM IMERG* is a new-generation satellite-based *P* dataset produced by combining passive microwave data, microwave-calibrated *IR* satellite data, and *P* gauge observations [31]. This dataset can be obtained from https://search.earthdata.nasa.gov/search?q=GPM_3IMERGM_06 (accessed on 31 October 2023). *TRMM 3B43* is a satellite-based *P* dataset combining *GPCC* rain gauge analysis [32]. It can be downloaded from https://search.earthdata.nasa.gov/search?q=TRMM_3B43 (accessed on 31 October 2023). *PERSIANN-CDR* is also a satellite-based *P* product, which can be obtained from <https://chrsdata.eng.uci.edu/> (accessed on 31 October 2023). *ERA5* is the reanalysis dataset, which estimates *P* by combining model simulation and rain gauge-based observations. Monthly reanalysis data of *ERA5* can be downloaded from <https://cds.climate.copernicus.eu/cdsapp#!/dataset/reanalysis-era5-single-levels?tab=form> (accessed on 31 October 2023). *GLDAS* is the global land data assimilation system. It estimates almost all budget fluxes, including *P*, *ET*, and *R*, based on land surface models such as the variable infiltration capacity (*VIC*). The *GLDAS* dataset can be downloaded from https://search.earthdata.nasa.gov/search?q=GLDAS_NOAH025_M_2.1 (accessed on 31 October 2023). Like *GLDAS*, *FLDAS* also estimates almost all budget components, including *P*, *ET*, and *R*, but not the state variable of *TWSC*. The product can be downloaded from https://search.earthdata.nasa.gov/search?q=FLDAS_NOAH01_C_GL_M (accessed on 31 October 2023).

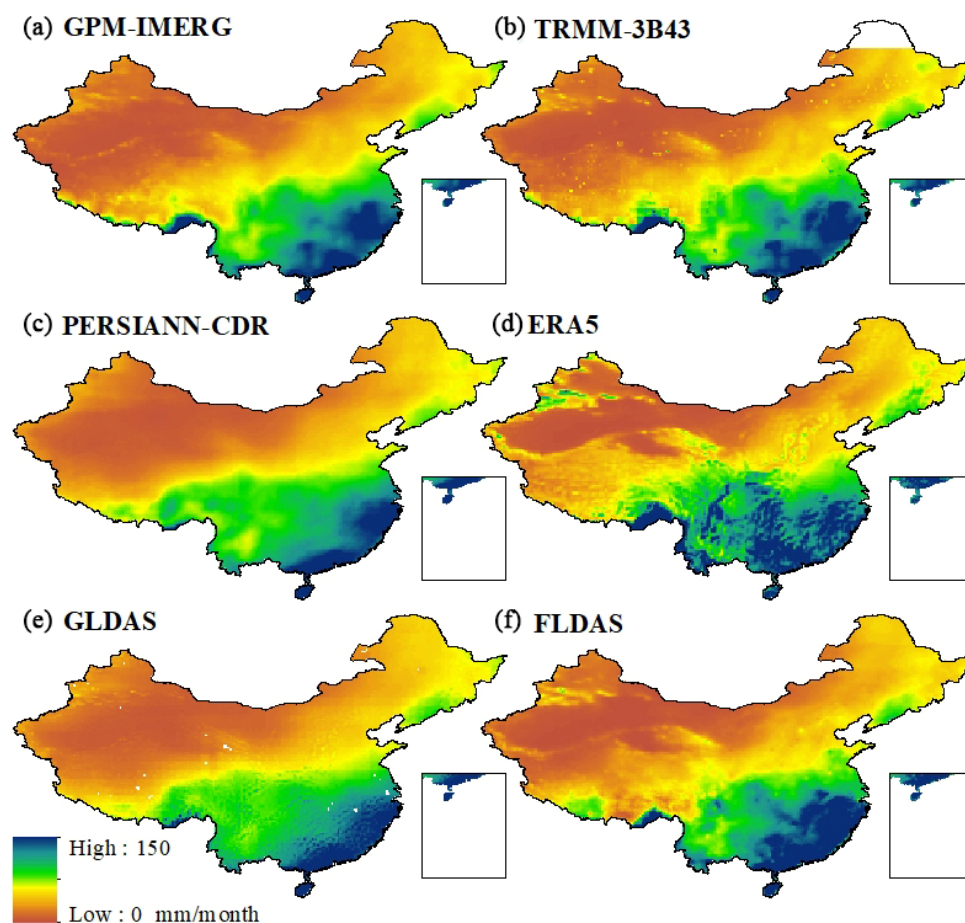


Figure 2. Spatial distribution of SRP products used in this study.

2.2.3. Datasets of Additional Budget Components

Together with P , the additional budget components of R , ET , and $TWSC$ jointly constitute a closed hydrological system. Both products, $GLDAS$ and $FLDAS$, provide global coverage of ET and runoff estimates. The R used in this study is the sum of the surface runoff and subsurface runoff simulated using hydrological models in $GLDAS$ and $FLDAS$. Since there are no sufficient $TWSC$ observations in most global basins, $GRACE$ $TWSC$ has been widely used for hydrological analysis in previous studies [19,37–39]. $GRACE$ satellite monitors $TWSC$ by mapping variations in the Earth's gravity field [40]. In this study, three $GRACE$ $TWSC$ products were considered: the CSR produced by U. Texas/Center for Space Research (Austin, TX, USA), GFZ produced by GeoForschungsZentrum Potsdam (Potsdam, Germany), and JPL produced by NASA Jet Propulsion Laboratory (Pasadena, CA, USA) [41]. These datasets cover the time period from 2002 to 2017 since the $GRACE$ mission was launched in March 2002 and finished in October 2017. The coarse spatial resolution of $GRACE$ $TWSC$ data (1 degree) determines that they are more suitable for $TWSC$ research in large-scale watersheds. Since these three $GRACE$ $TWSC$ products are produced by different centers, producing $TWSC$ data individually, their values may differ slightly. In most previous studies, they are commonly merged into one single $TWSC$ product to reduce uncertainties [25,42]. In this study, the data merging technology in Equation (8) below was used to merge these three $GRACE$ $TWSC$ products.

2.3. Methodology

Figure 3 shows the flowchart for assessing the water budget closure accuracy of SRP products relative to datasets of additional budget components. It mainly consists of three parts: (1) data preparation, (2) assessing the accuracy of SRP products by comparing them

with rain gauge-based observations using statistical methods for selecting high-precision datasets, and (3) assessing the water budget closure accuracy of the selected *SRP* products in combination with datasets of additional budget components using *BCMs*. The selection of high-precision datasets in step 2 ensures that the accuracy of *SRP* products applied to step 3 is high. In this study, we showed all results of the ΔRes in the Section 3 instead of only the ΔRes for the selected high-precision *SRP* products to intercompare the difference in closing water budget between satellite and reanalysis precipitation products.

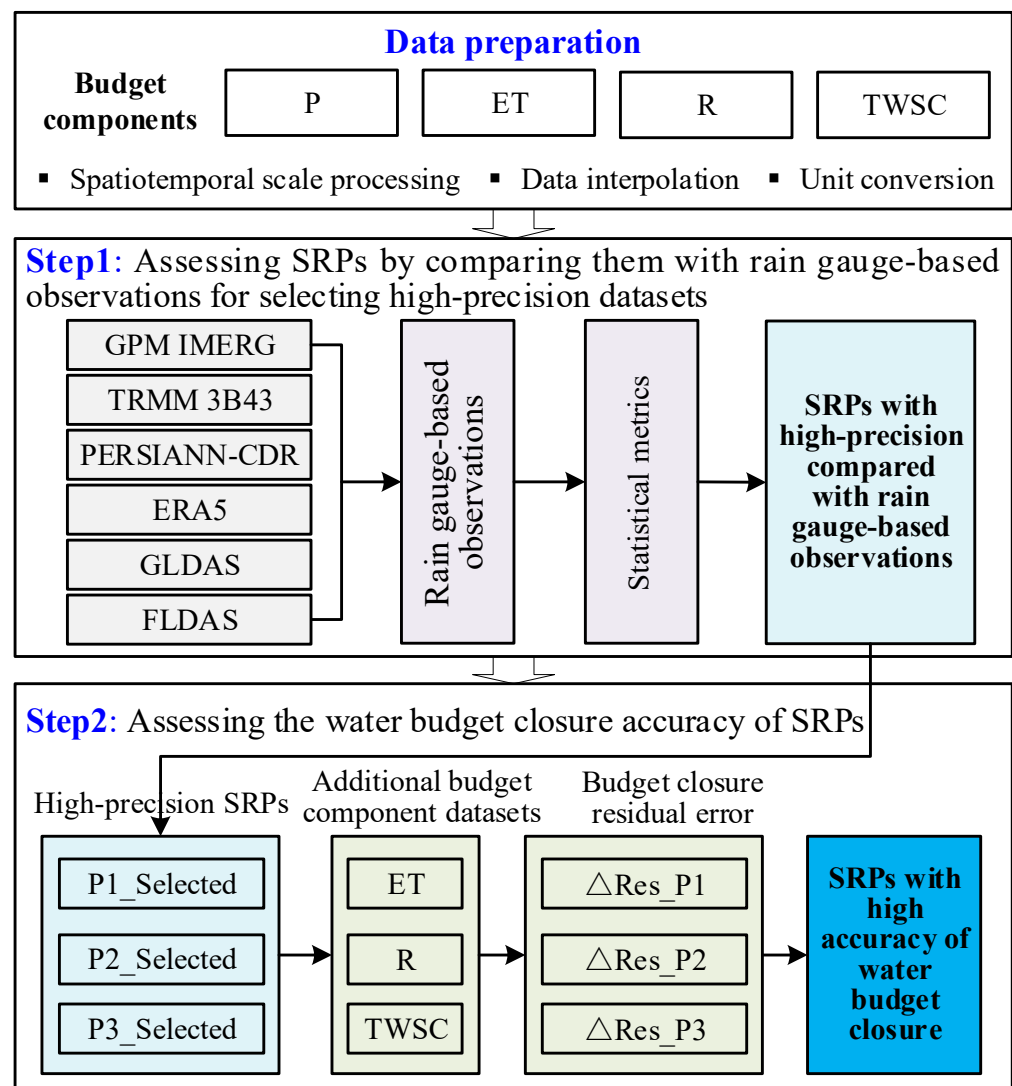


Figure 3. Framework for assessing the water budget closure accuracy of *SRP* products relative to datasets of additional budget components.

2.3.1. Data Preparation and Statistical Metrics

The datasets used in this study were pre-processed to form a unified format. In detail, all *SRP* products were mapped to a 1 degree spatial resolution and aggregated to a 1 month temporal resolution. We assess *SRP* products on a monthly timescale for the following reasons. The assessment of water budget closure requires datasets of four budget components (*P*, *ET*, *R*, and *TWSC*). However, *GRACE TWSC* datasets used in this study are monthly-based satellite observation data, constraining the study of water budget at finer scales. This is one of the main reasons why most current studies assess water budget only at a monthly time scale [12,13,16,25]. In addition, assessing the water budget at a time of less than a month will inevitably introduce more uncertainties because the water budget

quantifies all the water that flows into and out of the study area. It is difficult to estimate them at daily and hourly timescales accurately.

Three commonly used statistical metrics were employed to assess the accuracy of SRP products, including the root mean square error (RMSE), Pearson correlation coefficient (CC), and relative error (RE) [43,44]. The metrics CC, RMSE, and RE ranges are $[-1, 1]$, $[0, +\infty)$, $(-\infty, +\infty)$, respectively. The values of 1, 0, and 0, respectively, mean the best performance.

$$RMSE = \sqrt{\frac{\sum_{i=1}^n (Obs_i - Sim_i)^2}{n}} \quad (1)$$

$$CC = \frac{\sum_{i=1}^n (Obs_i - \overline{Obs})(Sim_i - \overline{Sim})}{\sqrt{\sum_{i=1}^n (Obs_i - \overline{Obs})^2} \sqrt{\sum_{i=1}^n (Sim_i - \overline{Sim})^2}} \quad (2)$$

$$RE = \frac{\sum_{i=1}^n (Sim_i - Obs_i)}{\sum_{i=1}^n Obs_i} \quad (3)$$

where n is the number of observed p values; Obs_i and Sim_i are the observed and estimated p values at time i , respectively; \overline{O} and \overline{S} are the averages of the observed and estimated p values, respectively.

2.3.2. Water Budget Closure Assessment

The general expression of the water budget equation is shown in Equation (4) [16,25]. Note that the monthly terrestrial water storage anomalies (TWSA) provided by GRACE are relative values (relative to the average in 2004–2009). Therefore, TWSA data in GRACE needs to be further processed to obtain TWSC data in Equation (4). In this study, the backward difference equation (Equation (5)) was used to deal with the gravity anomalies of the TWSA caused by GRACE sensors [17,18]. Accordingly, the budget components, except for the TWSC, were adjusted according to Equation (6) owing to the pre-processing of the GRACE TWSC products.

$$TWSC = P - ET - R \quad (4)$$

$$TWSC = \frac{TWSA(t+1) - TWSA(t)}{\Delta t} \quad (5)$$

$$\Delta W(t) = \left(\frac{P(t+1) + P(t)}{2} \right) - \left(\frac{ET(t+1) + ET(t)}{2} \right) - \left(\frac{R(t+1) + R(t)}{2} \right) \quad (6)$$

where $\Delta W(t)$ represents changes in water storage represented by the water budget flux terms P , ET , and R .

If all budget components in Equations (5) and (6) take “true values,” TWSC is equal to $\Delta W(t)$, that is, Equation (7) strictly holds. However, in practice, the water budget is rarely closed due to errors within the budget-component products. That is, the ΔRes error always exists in practice. According to previous studies, the ΔRes (due to errors in budget components) has been commonly used to assess the imbalance in the water budget [13,18]. It is calculated based on Equations (5) and (6). A small ΔRes represents high water budget closure accuracy, i.e., the high data consistency in the budget component products.

$$\Delta Res = TWSC - \Delta W(t) \quad (7)$$

The specific steps for assessing the water budget closure accuracy of SRP products relative to datasets of additional budget components are as follows. First, different water budget ensembles constituted by SRP products and the same products of additional budget components (ET , R , and $TWSC$) were formed (see Figure 3). Six SRP products were considered in this study. Assuming three were selected according to the first step: $P1_Selected$, $P2_Selected$, and $P3_Selected$. Therefore, three budget ensembles were formed in Figure 3: ΔRes_P1 , ΔRes_P2 , and ΔRes_P3 ; Second, we calculate and compare the ΔRes of budget ensembles for selecting high-precision SRP products with good water budget

closure relative to additional budget component products. Finally, *SRP* products with high accuracies in terms of both aspects of univariate (compared with rain gauge-based observations) and water budget closure (small ΔRes error) were determined.

There are two main error sources affecting water budget closure assessment using ΔRes , i.e., the error from products of additional budget components and the error from different *P* products. The ideal situation is that the accuracy of *SRP* products and additional budget component products, which are inputs for the ΔRes calculation, is high. For the former, there are no sufficient observations for each additional budget component at the global grid-scale due to the limited spatial distribution of ground observation sites. Therefore, observations of additional budget components cannot be directly applied to the calculation of the ΔRes . In addition, no single product for each budget component can capture the spatial pattern of the budget component for all regions of the globe [45]. To reduce the uncertainty of *SRP* assessment caused by products of additional budget components, the data merging technology in Equation (8) was used to derive hybrid estimates for each additional budget component since the merged values from multiple products have been shown to be close to observations and minimize data uncertainty [25,46].

$$Prod_x = \sum_{i=1}^n Prod_{x,i} \cdot \omega_i \quad \text{and} \quad \omega_i = \frac{\frac{1}{\sigma_i^2}}{\sum_{j=1}^n \frac{1}{\sigma_j^2}} \quad (8)$$

where $Prod_x$ denotes the merged value of budget component x , $Prod_{x,i}$ denotes the i -th budget component product, ω_i denotes the weight of the i -th product, σ_i^2 denotes the error variance of the i -th product, and n denotes the number of products for the budget component.

For the error from different *P* datasets, *SRP* products contain various sources of error due to the different *P* inversion algorithms and sensor sampling errors [11,47,48]. For example, *P* estimates from microwave sensors are based on microwave emission and scattering of raindrops and ice in low-frequency and high-frequency channels, respectively [4,11]. Reanalysis-based approaches are different from satellite inversion algorithms. They estimate *P* by combining rain gauge-based observations and climate model simulated data. Therefore, different data sources produce different errors in the estimation of *SRP* products. Moreover, the accuracy of *SRP* products varies between different regions [10]. In this study, we reduce the error caused by different data sources of *P* by selecting high-precision *SRP* products using statistical metrics.

3. Results

3.1. Assessment of *SRP* Products Using Statistic Metrics

This section focuses on assessing the accuracy of the selected six *SRP* products in mainland China. Figure 4 shows the spatial distribution of the statistical metrics *CC*, *RMSE*, and *RE*. For the metric *CC* (Figure 4a–f), all *SRP* products showed a better performance of *P* estimates in most eastern and southeastern regions of mainland China ($CC > 0.7$ for most stations) than the western regions ($CC < 0.7$ for most stations). *RE* (Figure 4m–r) showed the same spatial distribution as *CC*. According to Figure 1a, rain gauge stations were mainly distributed in China's eastern and southeastern regions. This may be one of the main reasons for the better estimates of *SRP* products in these regions. However, the metric *RMSE* in Figure 4g–l showed an opposite result compared with *CC* and *RE*. That is, *RMSE* with small values (≤ 30 mm), showing a better performance of *P* estimation, was mainly distributed in the western regions of mainland China. We speculate that this is mainly attributed to the smaller *P* magnitudes in western China (Figure 2), leading to a smaller difference in magnitude between *SRP* products and rain gauge-based observations.

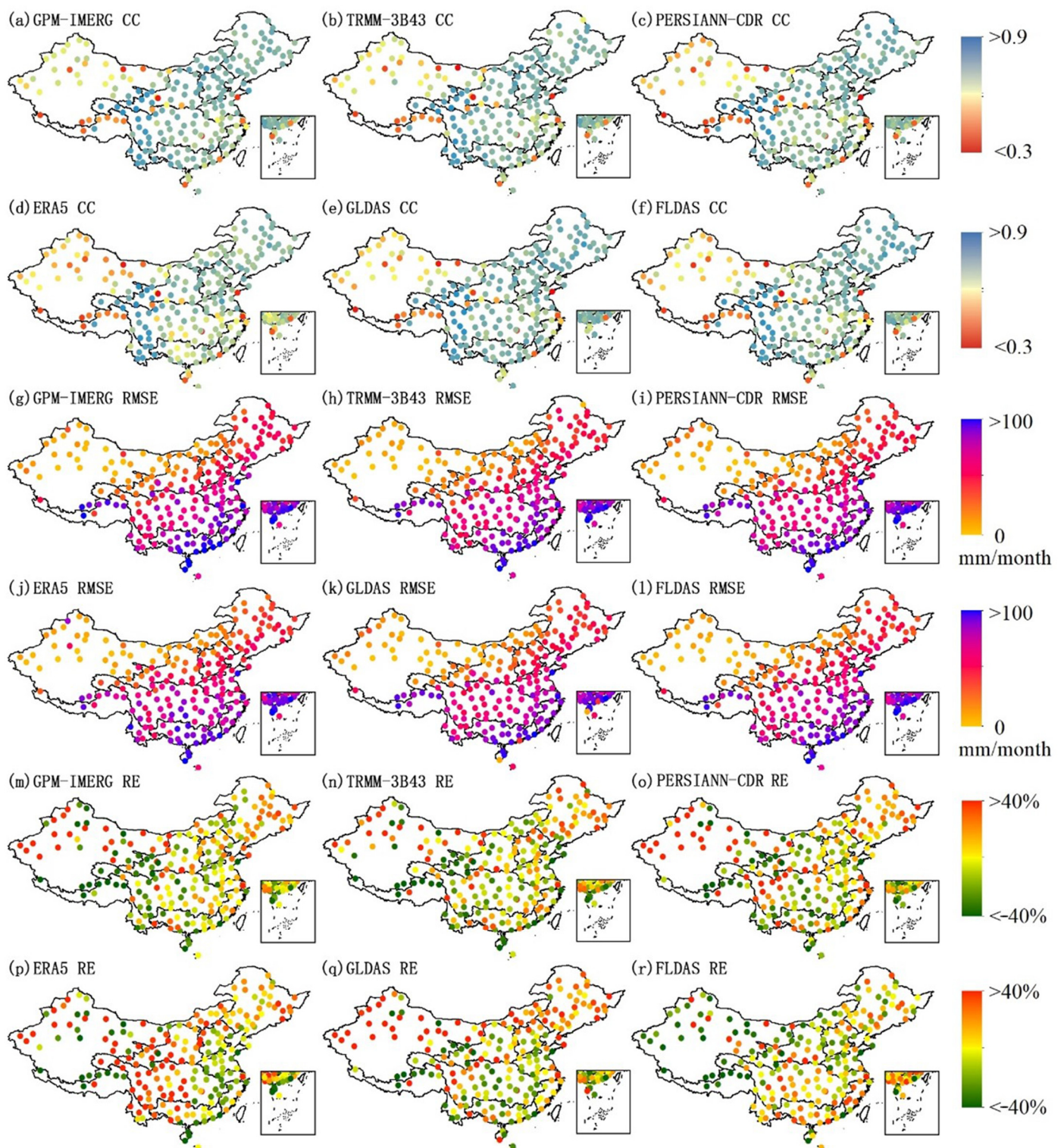


Figure 4. Spatial distribution of statistic metrics (*CC*, *RMSE*, and *RE*) at the monthly time scale in mainland China for assessing the accuracy of *SRP* products by comparing them with rain gauge-based observations at a point-to-pixel scale.

According to Figure 5, *GPM IMERG* showed a better performance of *P* estimation than *GLDAS*, *FLDAS*, and *TRMM 3B43* in mainland China, followed by *PERSIANN-CDR* and *ERA5*. Although the results of statistical metrics based on observations were reliable, the misestimates of *SRP* products caused by the information reuse of rain gauge-based

observations (the overlap in gauge-based observations used for producing and verifying SRP products) affected the accuracy of the results. Most SRP products, such as GPM IMERG, were combined with rain gauge-based observations during their production [31,49]. Therefore, it is very likely that the information of rain gauge stations used for bias correction or data fusion when producing SRP products was the same as that used for the performance assessment of SRP products using statistical metrics, resulting in information reuse errors. Some studies have shown that satellite-gauge products have higher P detection capabilities than satellite-only products [28]. Budget closure-based assessment methods can reduce the problem of data reuse for gauge-based observations to some extent, as they consider all budget components of P , ET , R , and $TWSC$ simultaneously rather than comparing them with observations. In addition, water budget closure has rarely been considered in the production of SRP products because of the lack of sensors capable of monitoring all budget components simultaneously [25].

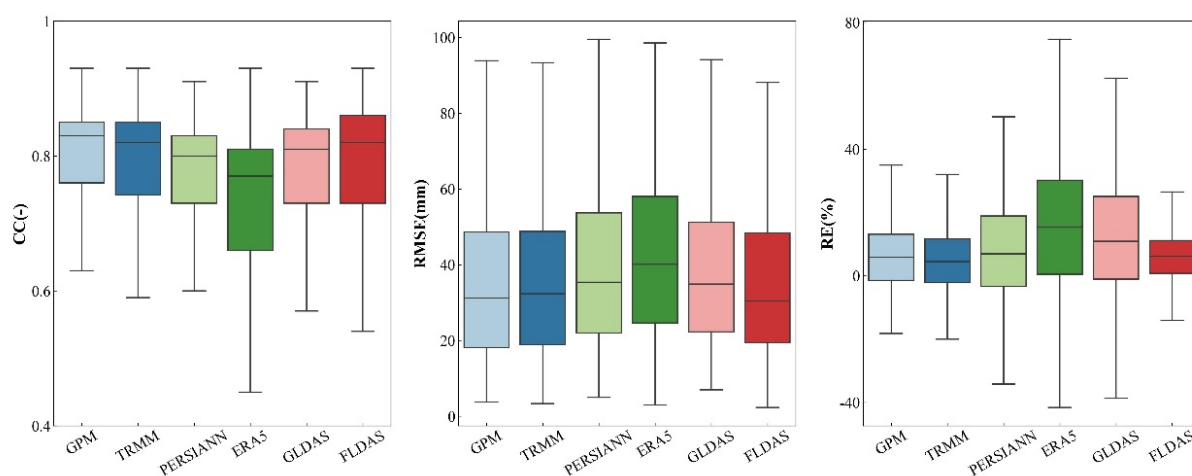


Figure 5. Statistical metrics for comparing the performance of different P products.

We compared the results with previous studies in mainland China. We reached the same conclusion as previous studies [44,47,50–54]. That is, GPM IMERG outperforms reanalysis products in mainland China. According to Jiang et al. [53], the performance of GPM IMERG is better than ERA5 over mainland China on the daily, monthly, and seasonal timescales. The results of Wei et al. [47] on the monthly timescale and Tang et al. [54] on the hourly timescale also showed the same results. All these studies indicated that reanalysis datasets (mainly referring to ERA5) tend to overestimate P against ground observations in many regions of China. A possible reason for GPM IMERG overperforming ERA5 in mainland China is that the former has been calibrated based on the monthly P products from GPCC (1.0° , monthly; Huffman et al. [55]) and daily P data from the Climate Prediction Center (CPC) (0.5° , daily; Mega et al. [56]), respectively (Xu et al. [47]; Jiang et al. [53]). However, ERA5 only assimilates the P estimates from the National Centers for Environment Prediction (NCEP) in the USA [57]. ERA5 products have not been calibrated based on P observations in mainland China [44]. It is worth mentioning that each SRP has its own strengths and weaknesses. The performance of SRP products varies with different regions (climatic zones), time scales, and precipitation phases [44]. It is difficult to find a product that performs well in all regions of the world [45].

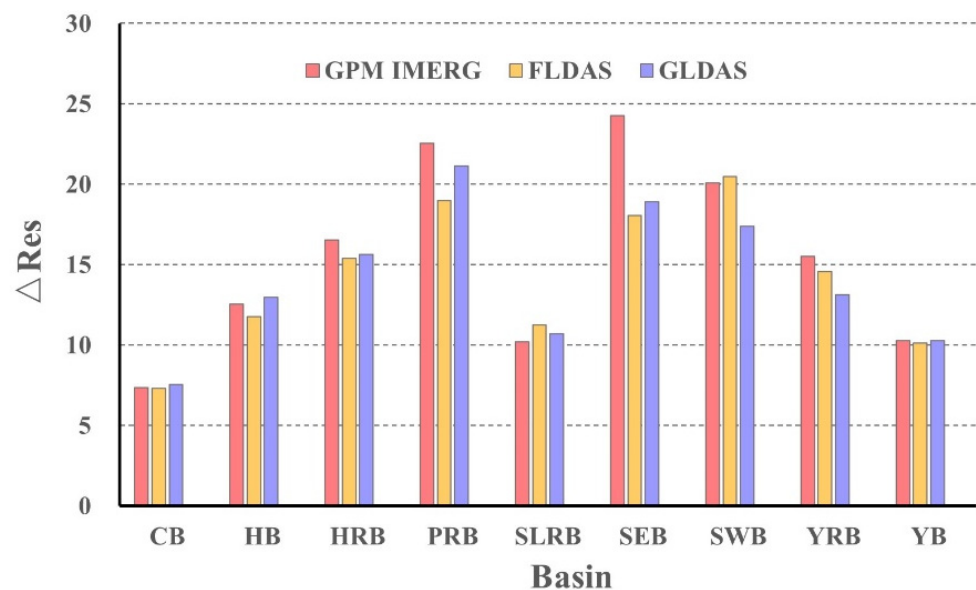
3.2. Water Budget Closure Assessment of SRP Products Relative to Additional Budget Component Products

This section focuses on assessing the water budget closure accuracy of SRP products relative to datasets of additional budget components on monthly and seasonal scales. Table 2 shows the monthly and seasonal average ΔRes . Note that the ΔRes in Table 2 is calculated based on different P products in Table 2 and the same merged ET , R , and $TWSC$ products in Section 2.2.3.

Table 2. Monthly and seasonal ΔRes of P products relative to additional budget components in mainland China.

Month	GPM-IMERG	TRMM-3B43	PERSIANN-CDR	ERA5	GLDAS	FLDAS
1	2.64	3.44	3.22	7.51	3.35	1.33
2	0.6	1.65	1.95	6.57	1.07	−0.2
3	−2.79	−1.29	−1.46	6.42	−1.42	−2.86
4	−2.26	−0.81	−0.91	10.49	0.32	−1.56
5	−4.25	−3.27	−2.11	11.29	−0.65	−2.71
6	−2.58	−2.17	0.88	13.95	2.2	−0.1
7	−14.69	−14.64	−8.18	3.26	−7.6	−8.89
8	−6.25	−6.76	1.54	14.01	2.54	2.44
9	−4.72	−5.23	−1.08	12.49	0.36	2.46
10	1.07	1.72	2.57	13.91	3.45	4.5
11	2.54	3.81	3.12	10.79	3.61	2.43
12	7.44	8.47	6.79	12.17	7.52	5.9
Spring	−9.52	−5.42	−4.89	27.72	−1.99	−6.85
Summer	−24.23	−23.06	−6.99	31.27	−4.76	−6.26
Autumn	−0.92	0.64	4.03	37.28	6.85	9.89
Winter	4.08	6.83	−0.53	22.23	5.35	0.85

According to Table 2, the monthly average ΔRes for SRP products over mainland China varied between ± 15 mm, which is acceptable based on previous studies that concluded that the value varies between ± 20 mm in most global basins [12,25,58]. Among the SRP products, GLDAS and FLDAS exhibited the best water budget closure relative to the selected datasets of additional budget components in Table 1, followed by GPM IMERG and TRMM 3B43, whereas PERSIANN-CDR and ERA5 exhibited the worse water budget closure. Therefore, BCMs showed a different result from that of statistical metrics, which indicates that GPM IMERG performed the best by comparing with rain gauge-based observations. This fully illustrates the importance of selecting high-precision SRP products using statistical metrics before assessing their water budget closure accuracy relative to datasets of additional budget components. Figure 6 shows the results of the ΔRes in nine major basins of mainland China. It shows that basins with large ΔRes values are HRB, PRB, SEB, and SWB. These basins are mainly distributed in the coastal areas of eastern and southern China, which are greatly affected by monsoon. The ΔRes in basins of YB, CB, and SLRB located in northern China is relatively small.

**Figure 6.** The ΔRes in different basins of mainland China.

The different results in the performance assessment of *SRP* products based on statistical methods and *BCMs* are mainly due to the different error sources of the two methods. For the accuracy of *SRP* products, it was assessed by comparing them with rain gauge-based observations using statistical metrics. Therefore, the results of *SRP* assessment are affected by the quality of rain gauge-based observations (e.g., the spatiotemporal coverage, data integrity, and record length of observed p values). However, the water budget closure assessment is affected by the data accuracy of *SRP* products and additional budget component products. Therefore, when we assess the water budget closure accuracy of *SRP* products, it is highly dependent on the selected datasets of additional budget components.

3.3. Monthly and Seasonal Variations of the ΔRes

Figure 7 shows the monthly variation of the ΔRes in mainland China, which is calculated based on *SRP* products and datasets of additional budget components. It is obvious that *ERA5* exhibited a clear overestimation of P compared with the remaining *SRP* products, as the ΔRes of *ERA5* was notably greater than zero in almost all the months (Figure 7). The high ΔRes for *ERA5* is caused by its high magnitude compared with the remaining *SRP* products. For the remaining ΔRes , they exhibited fluctuation changes. The Mann–Kendall (*MK*) method was used to test the significance of ΔRes changes. It is a non-parametric trend testing method. For the method, the sign of the statistic “ Z ” is used to determine whether the time series of ΔRes has a trend. When Z takes a positive value, it indicates an upward trend; on the contrary, it indicates a downward trend. When the absolute value of Z is greater than or equal to 1.64, 1.96, and 2.58, respectively, it means 90%, 95%, and 99% significance [59]. We perform the *MK* test using the Python software package. The Z -values for compositions *GPM IMERG*, *TRMM*, *PERSIANN*, *ERA5*, *GLDAS*, and *FLDAS* are -0.24 , -0.25 , 0.56 , -1.22 , 0.24 , and 0.27 , respectively. Therefore, the ΔRes for some compositions (*GPM IMERG*, *TRMM 3B43*, and *ERA5*) showed a decreasing trend over time in mainland China (mainly satellite products) and a slightly increasing trend for some other compositions (*GLDAS* and *FLDAS*, mainly reanalysis products). However, the decreasing and increasing trends are not significant since the absolute Z -values for all compositions are less than 1.64 (failed the 90% significance test). Many previous studies have also shown similar results. For example, Kinouchi et al. [22] reported a 0.03 mm/month increasing trend for residual errors according to their study in the Upper Chao Phraya River Basin.

The reduced ΔRes over time for *GPM IMERG* may be caused by the improved accuracy of *GPM IMERG* data. According to Tang et al. [54], the inversion accuracy of *GPM IMERG* significantly improved by comparing it with rain gauge-based observations because of the increasing number of passive microwave samples. According to Chen et al. (2020c), the *IMERG* Late Run performed slightly better in the estimation of global P than the *IMERG* Early Run. This shows that the improved accuracy of budget component products contributes to water budget closure. However, the decreasing trend of the ΔRes is not significant, which indicates that the development of satellite sensors and inversion algorithms pays more attention to the improvement of *SRP* inversion against rain gauge-based observations but lacks consideration of the water budget closure. Currently, no satellite sensor can monitor all budget components of hydrological systems simultaneously [25]. How to reduce the ΔRes error is the focus of further development of satellite hydrological data products. According to previous studies, some water budget closure correction methods, which focus on enforcing terrestrial water budget closure, have been proposed, such as the Proportional Redistribution, the Constrained Kalman Filter, the Multiple Collocation and the Minimized Series Deviation methods [13,24,41,54]. In addition, Luo et al. [6] proposed a method for balancing the terrestrial water budget and improving the estimation of individual budget components by combining existing water budget closure correction methods and observations of budget components. These methods can be further combined with P inversion/simulation algorithms for improving the water budget closure accuracy of P inversion in the future.

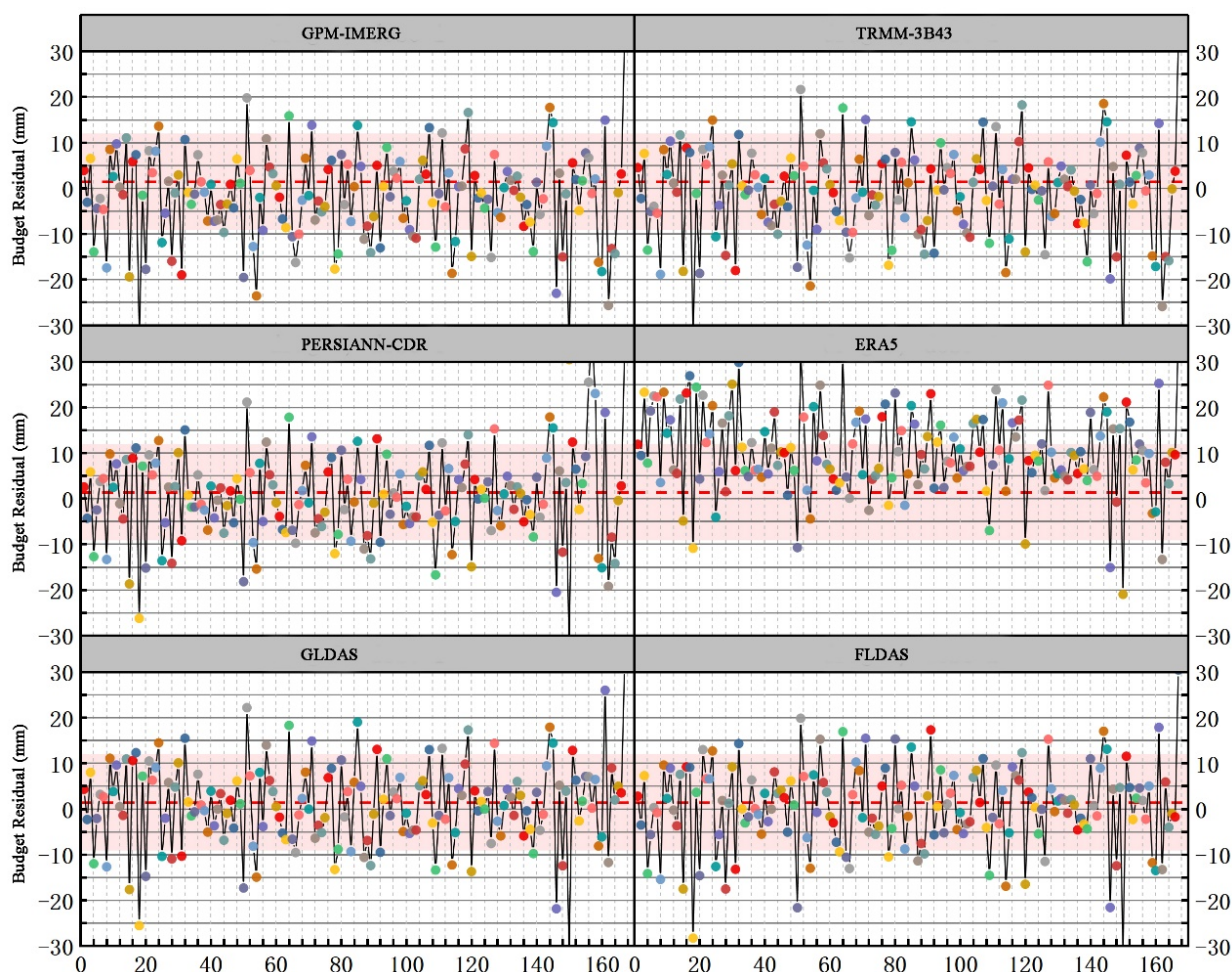


Figure 7. Temporal variation of the ΔRes from January 2003 to December 2016 for the selected SRP products in mainland China. The abscissa represents the month. There are 168 months from January 2003 to December 2016. For each sub-plot, the ΔRes is calculated based on the SRP in the corresponding sub-plot and datasets of additional budget components described in Section 2.2.3. Note that the ΔRes value at some time points exceeds the range of the ordinate (± 30 mm), with the absolute value changing between 30–40 mm. The large ΔRes at these time points is caused by the large negative TWSC. The colors used in the picture are meaningless.

Figure 8 shows the seasonal variation of the ΔRes in mainland China. According to Figure 8a, the monthly ΔRes varied between ± 20 mm. The ΔRes calculated based on reanalysis of SRP products (*PERSIANN*, *GLDAS*, and *FLDAS*) showed a smaller value than that calculated based on satellite SRP products (*GPM IMERG* and *TRMM 3B43*). The seasonal ΔRes (the sum of ΔRes values for three months corresponding to each season) in mainland China changed between ± 30 mm, except for the ΔRes calculated based on *ERA5*. The ΔRes for *PERSIANN*, *GLDAS*, and *FLDAS* also showed similar seasonal changes with a value smaller than that of other SRP products (absolute value). In the summer, the ΔRes calculated based on satellite SRP products showed high negative values. It showed positive values in autumn and winter. The ΔRes calculated based on reanalysis of SRP products showed high values in autumn.

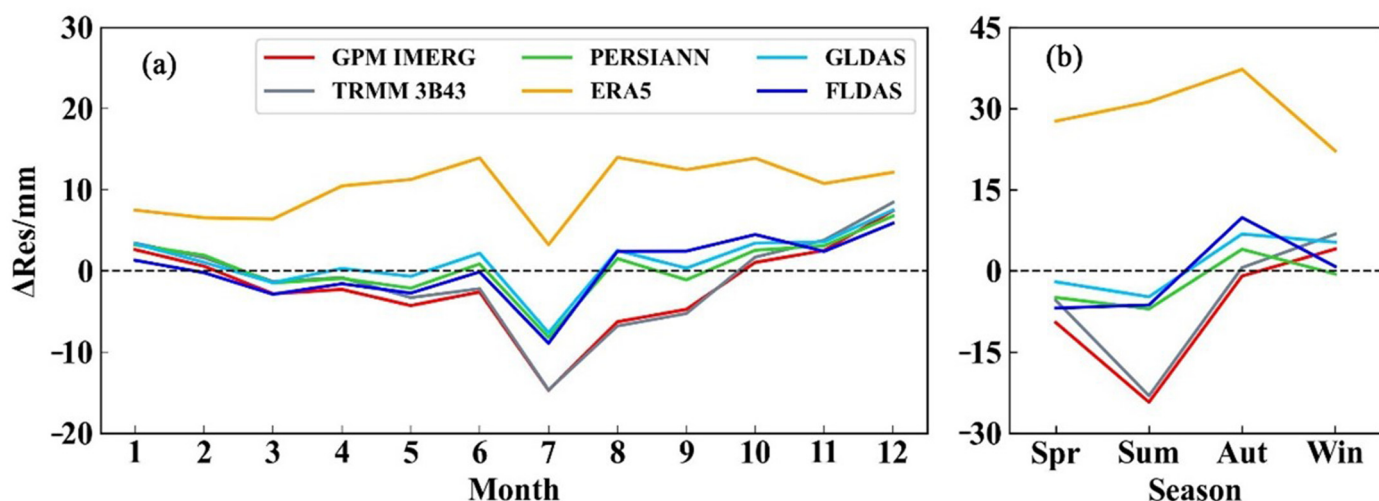


Figure 8. (a) Monthly variation of the ΔRes in mainland China. (b) Seasonal variation of the ΔRes in mainland China.

4. Discussion

Statistical methods and water budget closure-based methods assess the accuracy of *SRP* products from different perspectives, i.e., comparison with observations and the data consistency with datasets of additional budget components, respectively. The high accuracy of *SRP* products against observations based on statistical methods does not mean that their water budget closure accuracy is also high. The results of *SRP* evaluation in this study showed that water budget closure-based methods yielded a different result compared with statistical metrics. For the former, it showed a better performance for *GLDAS* and *FLDAS* than *GPM IMERG* and *TRMM 3B43*, followed by *PERSIANN-CDR* and *ERA5*. However, the latter showed a better performance for *GPM IMERG* than the remaining *SRP* products.

Regarding *SRP* assessment using statistical metrics, the improvement in the accuracy of *SRP* products is mainly caused by improved satellite sensors and inversion algorithms, and more importantly, many globally available *P* observations have been merged into *SRP* products using data assimilation technologies [60–62]. The performance of water budget closure is determined from the errors in all budget components, not just the error in the *P* variable. If the inversion accuracy of all budget components (meaning that all budget components are close to their “true” values) is improved, it can obtain a perfect water budget closure rather than a “false closure.” Therefore, previous studies on *SRP* inversion have focused mainly on improving the performance of *SRP* data against observations. Reducing the ΔRes error has received less attention. Developing integrated satellite sensors with abilities to monitor all budget components is critical for improving the accuracy of water budget closures, thereby laying the foundation for more accurate hydrological research [25].

According to this study, a combination of statistical methods and water budget closure-based methods provides an opportunity for selecting high-precision hydrological datasets. Combined with previous studies, we focus on a system summary of uncertainties that affect *SRP* assessment to provide insights into the further development of *SRP* assessment methods. The main sources of uncertainty include the inconsistent spatial and temporal resolution of budget component products, the quality of rain gauge-based observations, the selection of statistical metrics, and the errors in products of additional budget components [16,63].

Inconsistent spatial and temporal resolution of budget component datasets is a widely concerned issue in water budget closure assessment. The water budget involves four variables (*P*, *ET*, *R*, and *TWSC*). Their data are usually derived from different sources (observation sites, remote sensing, land surface models, and hydrological models), determining that they have different spatial and temporal resolutions [18,46]. Regardless of

which method (downscaling or upscaling) is used to deal with inconsistent data resolution, it inevitably introduces uncertainties, although the error introduced by upscaling is commonly less than that of downscaling. For statistical metrics, they represent different statistical significance and should be selected according to the research purpose and data availability of budget component observations [26,64]. Dense gauge networks facilitate the performance evaluation of *SRP* products [65]. However, observations often suffer from data integrity, length, and information reuse. The information reuse means that rain gauge-based observations merged into *SRP* products during their production are used again by users as a reference to assess the performance of these *SRP* products. Most *SRP* products, such as *GPM IMERG*, have merged with rain gauge-based observations during their production [31,49].

According to this study, the accuracy of water budget closure is highly related to errors in additional budget components. Methods that reduce uncertainties of additional budget components should be integrated with water budget closure assessment methods. For example, merged data from multiple products for each budget component performs better than one single product. This study assesses the water budget closure of *SRP* products relative to additional budget components by using the merged data of *GLDAS* and *FLDAS* for *ET* and *R* variables and merged data of three *GRACE TWSC* datasets for the *TWSC* variable.

5. Conclusions

Closing the water budget is critical for accurate hydrological research. This study focuses on assessing the accuracy of six popular *SRP* products in closing the water budget with respect to the selected datasets of additional budget components in mainland China by combining statistical methods and water budget closure-based methods. The integration of these two methods helps to obtain budget component datasets with high accuracy against observations and the small ΔRes . The main conclusions are as follows:

- (1) The ΔRes for reanalysis products of budget components is smaller than that of satellite products, although the accuracy of the latter is higher than the former when compared with ground-based observations. Combinations based on *GLDAS* and *FLDAS* showed a smaller ΔRes than *GPM IMERG* and *TRMM 3B43*. However, when compared with rain gauge-based observations, the accuracy of *GPM IMERG* and *TRMM 3B43* is higher than *GLDAS* and *FLDAS*.
- (2) In contrast to the results of statistical metrics, which showed an increasing accuracy of *SRP* products, the ΔRes for all combinations did not show a significant decreasing trend in mainland China. This implies that there was a lack of attention on water budget closure in the production of budget component products in previous studies, although it is critical for more accurate hydrological research and has attracted widespread attention recently.
- (3) The main error sources affecting the *SRP* assessment include the inconsistent spatial and temporal resolution of budget component datasets, the quality of rain gauge-based observations, the selection of statistical metrics, and the error in datasets of additional budget components. Methods that reduce uncertainties of budget components should be integrated with existing water budget closure assessment methods for reducing the uncertainties during water budget closure assessment.

Author Contributions: Conceptualization, Z.L. and H.L.; Methodology, Z.L., H.Y., H.L. and J.C.; Validation, Z.L. and H.Y.; Formal analysis, J.C.; Resources, H.L. and J.C.; Data curation, H.L.; Writing—original draft, Z.L.; Writing—review & editing, Z.L., H.L. and J.C.; Visualization, Z.L. and H.Y.; Supervision, Z.L., H.L. and J.C.; Funding acquisition, Z.L. All authors have read and agreed to the published version of the manuscript.

Funding: This research was supported by the Visiting Researcher Fund Program of the State Key Laboratory of Water Resources Engineering and Management (Grant No. 2022SWG04) and the National Natural Science Foundation of China (Grant No. 42201038, 52242905).

Data Availability Statement: The data used in this article can be obtained through the following website: <http://data.cma.cn/en> (accessed on 31 October 2023); https://search.earthdata.nasa.gov/search?q=GPM_3IMERGM_06 (accessed on 31 October 2023); https://search.earthdata.nasa.gov/search?q=TRMM_3B43 (accessed on 31 October 2023); <https://cds.climate.copernicus.eu/cdsapp#!/dataset/reanalysis-era5-single-levels?tab=form> (accessed on 2 November 2023); https://search.earthdata.nasa.gov/search?q=GLDAS_NOAH025_M_2.1 (accessed on 31 October 2023); https://search.earthdata.nasa.gov/search?q=FLDAS_NOAH01_C_GL_M (accessed on 31 October 2023).

Acknowledgments: We are very grateful to the journal editors and anonymous reviewers for their insightful comments and great efforts on this paper.

Conflicts of Interest: The authors declare no conflict of interest.

References

1. Forman, B.A.; Vivoni, E.R.; Margulis, S.A. Evaluation of ensemble-based distributed hydrologic model response with disaggregated precipitation products. *Water Resour. Res.* **2008**, *44*, 12. [CrossRef]
2. Bonan, D.B.; Siler, N.; Roe, G.H.; Armour, K.C. Energetic constraints on the pattern of changes to the hydrological cycle under global warming. *J. Clim.* **2023**, *36*, 3499–3522. [CrossRef]
3. Levizzani, V.; Cattani, E. Satellite remote sensing of precipitation and the terrestrial water cycle in a changing climate. *Remote Sens.* **2019**, *11*, 2301. [CrossRef]
4. Hong, Y.; Tang, G.; Ma, Y.; Huang, Q.; Han, Z.; Zeng, Z.; Yang, Y.; Wang, C.; Guo, X. Remote sensing precipitation: Sensors, retrievals, validations, and applications. In *Observation and Measurement of Ecohydrological Processes*; Springer: Berlin/Heidelberg, Germany, 2019; pp. 107–128.
5. Kim, J.; Han, H. Evaluation of the CMORPH high-resolution precipitation product for hydrological applications over South Korea. *Atmos. Res.* **2021**, *258*, 105650. [CrossRef]
6. Luo, Z.; Gao, Z.; Wang, L.; Wang, S.; Wang, L. A method for balancing the terrestrial water budget and improving the estimation of individual budget components. *Agric. For. Meteorol.* **2023**, *341*, 109667. [CrossRef]
7. Luo, Z.; Li, H.; Zhang, S.; Wang, L.; Wang, S.; Wang, L. A Novel Two-Step Method for Enforcing Water Budget Closure and an Intercomparison of Budget Closure Correction Methods Based on Satellite Hydrological Products. *Water Resour. Res.* **2023**, *59*, e2022WR032176. [CrossRef]
8. Ombadi, M.; Nguyen, P.; Sorooshian, S.; Hsu, K.-I. Developing Intensity-Duration-Frequency (IDF) Curves from Satellite-Based Precipitation: Methodology and Evaluation. *Water Resour. Res.* **2018**, *54*, 7752–7766. [CrossRef]
9. Sheffield, J.; Ferguson, C.R.; Troy, T.J.; Wood, E.F.; McCabe, M.F. Closing the terrestrial water budget from satellite remote sensing. *Geophys. Res. Lett.* **2009**, *36*, 07403. [CrossRef]
10. Amjad, M.; Yilmaz, M.T.; Yucel, I.; Yilmaz, K.K. Performance evaluation of satellite-and model-based precipitation products over varying climate and complex topography. *J. Hydrol.* **2020**, *584*, 124707. [CrossRef]
11. Moges, D.M.; Knoch, A.; Uuemaa, E. Application of satellite and reanalysis precipitation products for hydrological modeling in the data-scarce Porijõgi catchment, Estonia. *J. Hydrol. Reg. Stud.* **2022**, *41*, 101070. [CrossRef]
12. Luo, Z.; Shao, Q.; Wan, W.; Li, H.; Chen, X.; Zhu, S.; Ding, X. A new method for assessing satellite-based hydrological data products using water budget closure. *J. Hydrol.* **2021**, *594*, 125927. [CrossRef]
13. Pan, M.; Wood, E.F. Data assimilation for estimating the terrestrial water budget using a constrained ensemble kalman filter. *J. Hydrometeorol.* **2006**, *7*, 534–547. [CrossRef]
14. Dagan, G.; Stier, P.; Watson-Parris, D. Analysis of the atmospheric water budget for elucidating the spatial scale of precipitation changes under climate change. *Geophys. Res. Lett.* **2019**, *46*, 10504–10511. [CrossRef]
15. Lv, M.; Ma, Z.; Yuan, X.; Lv, M.; Li, M.; Zheng, Z. Water budget closure based on GRACE measurements and reconstructed evapotranspiration using GLDAS and water use data for two large densely-populated mid-latitude basins. *J. Hydrol.* **2017**, *547*, 585–599. [CrossRef]
16. Wang, S.; Huang, J.; Li, J.; Rivera, A.; McKenney, D.W.; Sheffield, J. Assessment of water budget for sixteen large drainage basins in Canada. *J. Hydrol.* **2014**, *512*, 1–15. [CrossRef]
17. Long, D.; Longuevergne, L.; Scanlon, B.R. Uncertainty in evapotranspiration from land surface modeling, remote sensing, and GRACE satellites. *Water Resour. Res.* **2014**, *50*, 1131–1151. [CrossRef]
18. Soltani, S.S.; Ataie-Ashtiani, B.; Danesh-Yazdi, M.; Simmons, C.T. A probabilistic framework for water budget estimation in low runoff regions: A case study of the central Basin of Iran. *J. Hydrol.* **2020**, *586*, 124898. [CrossRef]
19. Rodell, M.; Reager, J.T. Water cycle science enabled by the GRACE and GRACE-FO satellite missions. *Nat. Water* **2023**, *1*, 47–59. [CrossRef]
20. Hobeichi, S.; Abramowitz, G.; Evans, J. Conserving Land–Atmosphere Synthesis Suite (CLASS). *J. Clim.* **2020**, *33*, 1821–1844. [CrossRef]
21. Lehmann, F.; Vishwakarma, B.D.; Bamber, J. How well are we able to close the water budget at the global scale? *Hydrol. Earth Syst. Sci.* **2022**, *26*, 35–54. [CrossRef]

22. Abhishek Kinouchi, T.; Abolafia-Rosenzweig, R.; Ito, M. Water budget closure in the Upper Chao Phraya River basin, Thailand using multisource data. *Remote Sens.* **2021**, *14*, 173. [[CrossRef](#)]
23. Gao, H.; Tang, Q.; Ferguson, C.R.; Wood, E.F.; Lettenmaier, D.P. Estimating the water budget of major US river basins via remote sensing. *Int. J. Remote Sens.* **2010**, *31*, 3955–3978. [[CrossRef](#)]
24. Abolafia-Rosenzweig, R.; Pan, M.; Zeng, J.L.; Livneh, B. Remotely sensed ensembles of the terrestrial water budget over major global river basins: An assessment of three closure techniques. *Remote Sens. Environ.* **2021**, *252*, 112191. [[CrossRef](#)]
25. Sahoo, A.K.; Pan, M.; Troy, T.J.; Vinukollu, R.K.; Sheffield, J.; Wood, E.F. Reconciling the global terrestrial water budget using satellite remote sensing. *Remote Sens. Environ.* **2011**, *115*, 1850–1865. [[CrossRef](#)]
26. Hamed, M.M.; Nashwan, M.S.; Shahid, S. Performance evaluation of reanalysis precipitation products in Egypt using fuzzy entropy time series similarity analysis. *Int. J. Climatol.* **2021**, *41*, 5431–5446. [[CrossRef](#)]
27. Chen, H.; Yong, B.; Shen, Y.; Liu, J.; Hong, Y.; Zhang, J. Comparison analysis of six purely satellite-derived global precipitation estimates. *J. Hydrol.* **2020**, *581*, 124376. [[CrossRef](#)]
28. Zhou, Z.; Guo, B.; Xing, W.; Zhou, J.; Xu, F.; Xu, Y. Comprehensive evaluation of latest GPM era IMERG and GSMaP precipitation products over mainland China. *Atmos. Res.* **2020**, *246*, 105132. [[CrossRef](#)]
29. Pan, M.; Li, H.; Wood, E. Assessing the skill of satellite-based precipitation estimates in hydrologic applications. *Water Resour. Res.* **2010**, *46*, 9. [[CrossRef](#)]
30. Bouizrou, I.; Bouadila, A.; Aqnouy, M.; Gourfi, A. Assessment of remotely sensed precipitation products for climatic and hydrological studies in arid to semi-arid data-scarce region, central-western Morocco. *Remote Sens. Appl. Soc. Environ.* **2023**, *30*, 100976. [[CrossRef](#)]
31. Huffman, G.J.; Stocker, E.F.; Bolvin, D.T.; Nelkin, E.J.; Tan, J. *GPM IMERG Final Precipitation L3 Half Hourly 0.1 Degree x 0.1 Degree V06*; Goddard Earth Sciences Data and Information Services Center (GES DISC): Greenbelt, MD, USA, 2019.
32. Huffman, G.J.; Adler, R.F.; Bolvin, D.T.; Nelkin, E.J. The TRMM Multi-Satellite Precipitation Analysis (TMPA). In *Satellite Rainfall Applications for Surface Hydrology*; Gebremichael, M., Hossain, F., Eds.; Springer: Dordrecht, The Netherlands, 2010; pp. 3–22.
33. Ashouri, H.; Hsu, K.L.; Sorooshian, S.; Braithwaite, D.K.; Knapp, K.R.; Cecil, L.D.; Nelson, B.R.; Prat, O.P. PERSIANN-CDR: Daily precipitation climate data record from multisatellite observations for hydrological and climate studies. *Bull. Am. Meteorol. Soc.* **2015**, *96*, 69–83. [[CrossRef](#)]
34. Copernicus Climate Change Service (C3S). *ERA5: Fifth Generation of ECMWF Atmospheric Reanalysis of the Global Climate*; Copernicus Climate Change Service Climate Data Store (CDS): Frankfurt, Germany, 2017.
35. Rodell, M.; Houser, P.R.; Jambor UE, A.; Gottschalck, J.; Mitchell, K.; Meng, C.J.; Arsenault, K.; Cosgrove, B.; Radakovich, J.; Bosilovich, M.; et al. The global land data assimilation system. *Bull. Am. Meteorol. Soc.* **2004**, *85*, 381–394. [[CrossRef](#)]
36. McNally, A.; Arsenault, K.; Kumar, S.; Shukla, S.; Peterson, P.; Wang, S.; Funk, C.; Peters-Lidard, C.D.; Verdin, J.P. A land data assimilation system for sub-Saharan Africa food and water security applications. *Sci. Data* **2017**, *4*, 170012. [[CrossRef](#)] [[PubMed](#)]
37. Mehrnegar, N.; Schumacher, M.; Jagdhuber, T.; Forootan, E. Making the Best Use of GRACE, GRACE-FO and SMAP Data through a Constrained Bayesian Data-Model Integration. *Water Resour. Res.* **2023**, *59*, e2023WR034544. [[CrossRef](#)]
38. Li, B.; Rodell, M.; Zaitchik, B.F.; Reichle, R.H.; Koster, R.D.; van Dam, T.M. Assimilation of GRACE terrestrial water storage into a land surface model: Evaluation and potential value for drought monitoring in western and central Europe. *J. Hydrol.* **2012**, *446*, 103–115. [[CrossRef](#)]
39. Schulze, K.; Kusche, J.; Gerdener, H.; Engels, O.; Döll, P.; Müller Schmied, H.; Sebastian, A.; Shadkam, S. Joint assimilation of GRACE Total Water Storage Anomalies and In-Situ Streamflow Data into a Global Hydrological Model. In Proceedings of the EGU General Assembly Conference Abstracts, Vienna, Austria, 23–27 May 2022; p. p. EGU22–5321.
40. Sun, A.Y.; Scanlon, B.R.; Save, H.; Rateb, A. Reconstruction of GRACE Total Water Storage Through Automated Machine Learning. *Water Resour. Res.* **2021**, *57*, e2020WR028666. [[CrossRef](#)]
41. Munier, S.; Aires, F.; Schlaffer, S.; Prigent, C.; Papa, F.; Maisongrande, P.; Pan, M. Combining data sets of satellite-retrieved products for basin-scale water balance study: 2. Evaluation on the Mississippi Basin and closure correction model. *J. Geophys. Res.-Atmos.* **2014**, *119*, 12100–12116. [[CrossRef](#)]
42. Zhang, Y.; Pan, M.; Sheffield, J.; Siemann, A.L.; Fisher, C.K.; Liang, M.; Beck, H.E.; Wanders, N.; MacCracken, R.F.; Houser, P.R. A Climate Data Record (CDR) for the global terrestrial water budget: 1984–2010. *Hydrol. Earth Syst. Sci.* **2018**, *22*, 241–263. [[CrossRef](#)]
43. Pradhan, A.; Indu, J. Assessment of SM2RAIN derived and IMERG based precipitation products for hydrological simulation. *J. Hydrol.* **2021**, *603*, 127191. [[CrossRef](#)]
44. Xu, J.; Ma, Z.; Yan, S.; Peng, J. Do ERA5 and ERA5-land precipitation estimates outperform satellite-based precipitation products? A comprehensive comparison between state-of-the-art model-based and satellite-based precipitation products over mainland China. *J. Hydrol.* **2022**, *605*, 127353. [[CrossRef](#)]
45. Chen, S.; Xiong, L.; Ma, Q.; Kim, J.-S.; Chen, J.; Xu, C.-Y. Improving daily spatial precipitation estimates by merging gauge observation with multiple satellite-based precipitation products based on the geographically weighted ridge regression method. *J. Hydrol.* **2020**, *589*, 125156. [[CrossRef](#)]
46. Yao, Y.; Liang, S.; Xie, X.; Cheng, J.; Jia, K.; Li, Y.; Liu, R. Estimation of the terrestrial water budget over northern China by merging multiple datasets. *J. Hydrol.* **2014**, *519*, 50–68. [[CrossRef](#)]

47. Wei, L.; Jiang, S.; Ren, L.; Wang, M.; Zhang, L.; Liu, Y.; Yuan, F.; Yang, X. Evaluation of seventeen satellite-, reanalysis-, and gauge-based precipitation products for drought monitoring across mainland China. *Atmos. Res.* **2021**, *263*, 105813. [[CrossRef](#)]
48. Chaudhary, S.; Dhanya, C.T. An improved error decomposition scheme for satellite-based precipitation products. *J. Hydrol.* **2021**, *598*, 126434. [[CrossRef](#)]
49. Pradhan, R.K.; Markonis, Y.; Vargas Godoy, M.R.; Villalba-Pradas, A.; Andreadis, K.M.; Nikolopoulos, E.I.; Papalexiou, S.M.; Rahim, A.; Tapiador, F.J.; Hanel, M. Review of GPM IMERG performance: A global perspective. *Remote Sens. Environ.* **2022**, *268*, 112754. [[CrossRef](#)]
50. Liu, Z.; Di, Z.; Qin, P.; Zhang, S.; Ma, Q. Evaluation of Six Satellite Precipitation Products over the Chinese Mainland. *Remote Sens.* **2022**, *14*, 6277. [[CrossRef](#)]
51. Fang, J.; Yang, W.; Luan, Y.; Du, J.; Lin, A.; Zhao, L. Evaluation of the TRMM 3B42 and GPM IMERG products for extreme precipitation analysis over China. *Atmos. Res.* **2019**, *223*, 24–38. [[CrossRef](#)]
52. He, Q.; Yang, J.; Chen, H.; Liu, J.; Ji, Q.; Wang, Y.; Tang, F. Evaluation of extreme precipitation based on three long-term gridded products over the Qinghai-Tibet Plateau. *Remote Sens.* **2021**, *13*, 3010. [[CrossRef](#)]
53. Jiang, S.H.; Wei, L.Y.; Ren, L.L.; Zhang, L.Q.; Wang, M.H.; Cui, H. Evaluation of IMERG, TMPA, ERA5, and CPC precipitation products over mainland China: Spatiotemporal patterns and extremes. *Water Sci. Eng.* **2023**, *16*, 45–56. [[CrossRef](#)]
54. Tang, G.; Clark, M.P.; Papalexiou, S.M.; Ma, Z.; Hong, Y. Have satellite precipitation products improved over last two decades? A comprehensive comparison of GPM IMERG with nine satellite and reanalysis datasets. *Remote Sens. Environ.* **2020**, *240*, 111697. [[CrossRef](#)]
55. Huffman, G.J.; Bolvin, D.T.; Braithwaite, D.; Hsu, K.L.; Joyce, R.J.; Kidd, C.; Nelkin, E.J.; Sorooshian, S.; Stocker, E.F.; Tan, J.; et al. Integrated multi-satellite retrievals for the global precipitation measurement (GPM) mission (IMERG). *Satell. Precip. Meas.* **2020**, *1*, 343–353.
56. Mega, T.; Ushio, T.; Takahiro, M.; Kubota, T.; Kachi, M.; Oki, R. Gauge-adjusted global satellite mapping of precipitation. *IEEE Trans. Geosci. Remote Sens.* **2018**, *57*, 1928–1935. [[CrossRef](#)]
57. Hersbach, H.; Bell, B.; Berrisford, P.; Hirahara, S.; Horányi, A.; Muñoz-Sabater, J.; Nicolas, J.; Peubey, C.; Radu, R.; Schepers, D.; et al. The ERA5 global reanalysis. *Q. J. R. Meteorol. Soc.* **2020**, *146*, 1999–2049. [[CrossRef](#)]
58. Kurkute, S.; Li, Z.; Li, Y.; Huo, F. Assessment and projection of the water budget over western Canada using convection-permitting weather research and forecasting simulations. *Hydrol. Earth Syst. Sci.* **2020**, *24*, 3677–3697. [[CrossRef](#)]
59. Nundy, S.; Kakar, A.; Bhutta, Z.A. How to calculate an adequate sample size? How to Practice Academic Medicine and Publish from Developing Countries? *A Pract. Guide* **2022**, 81–93. [[CrossRef](#)]
60. Nashwan, M.S.; Shahid, S.; Dewan, A.; Ismail, T.; Alias, N. Performance of five high resolution satellite-based precipitation products in arid region of Egypt: An evaluation. *Atmos. Res.* **2020**, *236*, 104809. [[CrossRef](#)]
61. Derin, Y.; Yilmaz, K.K. Evaluation of Multiple Satellite-Based Precipitation Products over Complex Topography. *J. Hydrometeorol.* **2014**, *15*, 1498–1516. [[CrossRef](#)]
62. Li, X.; Zhang, Q.; Xu, C.-Y. Assessing the performance of satellite-based precipitation products and its dependence on topography over Poyang Lake basin. *Theor. Appl. Climatol.* **2014**, *115*, 713–729. [[CrossRef](#)]
63. Oliveira, P.T.S.; Nearing, M.A.; Moran, M.S.; Goodrich, D.C.; Wendland, E.; Gupta, H.V. Trends in water balance components across the Brazilian Cerrado. *Water Resour. Res.* **2014**, *50*, 7100–7114. [[CrossRef](#)]
64. Wang, Q.; Xia, J.; She, D.; Zhang, X.; Liu, J.; Zhang, Y. Assessment of four latest long-term satellite-based precipitation products in capturing the extreme precipitation and streamflow across a humid region of southern China. *Atmos. Res.* **2021**, *257*, 105554. [[CrossRef](#)]
65. Lei, H.; Li, H.; Zhao, H.; Ao, T.; Li, X. Comprehensive evaluation of satellite and reanalysis precipitation products over the eastern Tibetan plateau characterized by a high diversity of topographies. *Atmos. Res.* **2021**, *259*, 105661. [[CrossRef](#)]

Disclaimer/Publisher’s Note: The statements, opinions and data contained in all publications are solely those of the individual author(s) and contributor(s) and not of MDPI and/or the editor(s). MDPI and/or the editor(s) disclaim responsibility for any injury to people or property resulting from any ideas, methods, instructions or products referred to in the content.